PREDICTION OF DIAPHRAGM DISPLACEMENT

Robert H. Falk
Research Engineer
USDA Forest Service
Forest Products Laboratory
Madison, WI 53705-2398

Rafik Y. Itani
Professor
Civil and Environmental Engineering
Washington State University
Pullman, WA 99164-2914

Abstract

This paper describes a two-dimensional finite element model for analyzing vertical and horizontal wood diaphragms. Central to the development of this model is the formulation of a nonlinear finite element that accounts for the distribution and stiffness of fasteners connecting the sheathing to the framing. A 16- by 48-ft horizontal diaphragm is analyzed with the model, and comparisons are made to displacements computed with a commonly used diaphragm deflection equation.

Introduction

Diaphragms are important components of wood-framed buildings that are used to resist and transfer the lateral shear forces produced by wind or earthquakes. Although considerable analytical research has been performed on wood diaphragms, it has primarily concentrated on the modeling of wall behavior. Few models have been used to address the behavior of other types of diaphragms, such as floors and ceilings.

The purpose of this paper is to present the formulation of a nonlinear finite element used to represent the distribution and stiffness of the nails that secure sheathing to framing in a wood diaphragm. When linked with conventional beam and plane stress elements, which represent diaphragm framing and sheathing, respectively, the resulting model can be used to analyze a variety of diaphragms (walls, floors, and ceilings) with different geometry and loading arrangement.

The ability of the model to predict displacements is investigated through the analysis of a 16- by 48-ft horizontal diaphragm. Analysis results are compared to results derived from a commonly used deflection equation.

Related Research

Though research on wood diaphragms dates back to 1927 (9), most of the research until the 1960's was experimental in nature and focused on the relative influence of parameters such as sheathing type and orientation, fastener type and spacing, and diaphragm geometry. Several mathematical models for wood diaphragm analysis have since been proposed. In 1967, Amana and Booth published the results of theoretical studies on nailed and glued plywood stressed-skin components (1). The concept of nail modulus to account for fastener stiffness was first presented in this paper. Foschi presented a more general nonlinear finite element model in 1977 for predicting the displacements of a 20- by 60-ft roof diaphragm (6). In 1978, Tuomi and McCutcheon described a model for predicting racking resistance of wood stud walls (11). Experimental test data and theoretical results were in good agreement. Although this model was limited to linear nail slip, it has since been modified to account for fastener nonlinearity (8).

Formulas for analyzing wood-frame shear walls with sheathing attached by discrete fasteners were presented by Easley et al. in 1982 (4). Expressions were derived for sheathing fastener forces, linear shear stiffness, and nonlinear shear load-strain behavior. Eight 8- by 12-ft plywood-sheathed walls were tested for model verification.

Itani and Cheung presented a finite element model in 1984 for the static analysis of wood diaphragms (7). A single line of fasteners can be represented with the developed joint element, which accounts for nonlinear nail-slip properties. This model does not impose restrictions on sheathing arrangement, load application, or diaphragm geometry. However, we found that the model required an excessive amount of computer time for the analysis of larger diaphragms. A more efficient formulation with improved representation of the fasteners was clearly needed. The model described in this paper is the result.

Finite Element Formulation

Wood diaphragms are constructed from three basic elements: frame members (studs or joists), sheathing (plywood, particleboard, or gypsumboard), and fasteners (nails or staples). Figure 1 shows a typically constructed floor diaphragm. The finite element developed in the following formulation represents the distribution and stiffness of nail fasteners connecting sheathing panels and lumber framing in a wall, floor, ceiling, or roof diaphragm. This element will be referred to as a transfer element since it accounts for the transfer of lateral force through the fasteners from the sheathing to the framing (and vice versa).

The transfer element accounts for the stiffness of individual fasteners through the use of spring pairs, which can deform nonlinearly (4). Linking of the transfer element with conventional beam and plane stress isoparametric elements, which are used to model the lumber framing and sheathing panels, respectively, allows analysis of an entire diaphragm subject to lateral loads. The stiffness of the transfer element is established through the summation of the stiffnesses of the individual fasteners. Fastener stiffness is determined from the slope of the nonlinear load-displacement curve for the type of fastener modeled. A single transfer element can represent multiple lines of fasteners. Typically, a transfer element is sized to match the dimensions of the sheathing element to which it connects (accounting for all the fasteners connecting that sheathing panel to the framing).

Since the transfer element is linked between a single sheathing element and at least four beam elements, the number of nodes and the resulting number of degrees of freedom (DOF) needed to describe the transfer element are dictated only by its connection to these elements, not by the number of fasteners it represents. Previous formulations accounted for a single fastener or a single line of fasteners (4,6,7). The utilization of multiple rows and columns of fasteners in a single transfer element significantly reduces the DOF required for diaphragm analysis and increases computational efficiency. This increase in efficiency is important for the analysis of large horizontal diaphragms.

Figure 2 shows the node numbers, DOF, and coordinate orientation of the transfer element. Height H and width W are variables dependent on the dimensions of the attached sheathing element. Although offset in the figure for clarity, nodes 1 to 4 have the same undisplaced coordinates as nodes 5 to 8, respectively. Nodes 1 to 4 link to beam elements, and nodes 5 to 8 link to the single sheathing element. Since beam elements possess three DOF per node and the plane stress isoparametric element used to model the sheathing possesses 2 DOF per node, the transfer element requires a total of 20 DOF.

Although the spring pairs have zero length before displacement, the magnitude of displacement depends on the relative displacement of the beam and sheathing elements to which the transfer element is attached. In Figure 3, the relative displacement is described by the solid and dashed lines between the nodes of the transfer element. To assure compatibility, these functions are identical to the functions used to describe the beam and sheathing element displacement (Table 1, column 1).

The functions that describe the displacement of spring pairs are listed in Table 1. For example, $d_{1x}(y)$ describes the displacement of each spring pair as a result of displacement at node 1 in the x direction. The terms a_j refer to the location of a spring pair as a ratio of its y coordinate and the transfer element height H (Table 1, left-hand column).

Since the expressions d_{1x} to d_{8y} describe the variation of spring pair displacement only in terms of the height of the element, similar functions are needed to describe spring pair displacement across the element width. These functions, c_{1x} to c_{8y}, are given in column 2 of Table 1. Note that the functions are linear, which is a reasonable assumption of the change in spring pair displacement across the transfer element. The terms b_i describe the x coordinate of a spring pair as a ratio of the transfer element width W.

The terms a_j and b_i define the location of a spring pair anywhere on the x-y plane of the transfer element. Nails on the perimeter of sheathing panels as well as interior (field) nails with different spacings can be represented.

To develop the stiffness matrix of the transfer element, unit displacements are applied to each DOF. Forces resulting at each DOF, caused by the displacement of all the spring pairs within the element, are summed to obtain the coefficients of the transfer element stiffness matrix.

The spring force associated with each spring pair is obtained as a product of the nonlinear spring stiffness k_{ij} and the corresponding spring displacements; k_{ij} is determined from the slope of the fastener load-displacement curve at the k_{ij} spring displacement level.

The force f in spring pair ij, caused by a unit displacement at node 1 in the x direction, is expressed as

$$f_{1x,ijx} = k_{ij} d_{1x} c_{1x} \qquad [1]$$

The subscripts of f indicate the node number and the direction of the unit displacement (1x) as well as the spring location and the direction of force (ijx). The subscripts of d and c indicate the node number and direction of the unit displacement (1x).

To determine the coefficients of the transfer element stiffness matrix, the resultant spring pair force at each DOF caused by unit displacement at each node must be determined. This nodal force S is equal to the sum of the product of the force in each spring pair and the corresponding function value describing spring pair displacement. For example, the resultant force at node 2 in the x direction, caused by a unit displacement applied at node 1 in the x direction, is expressed as

$$S_{2x,1x} = \sum_{i=1}^{n} \sum_{j=1}^{m} f_{1x,ijx}\, d_{2x}\, c_{2x} \qquad [2]$$

Note that the total number of spring pairs in columns and rows in the x-y plane are represented by n and m, respectively. Substituting the expression for spring force (Eq. [1]) into Equation [2] gives

$$S_{2x,1x} = \sum_{i=1}^{n} \sum_{j=1}^{m} k_{ij}\, d_{1x}\, c_{1x}\, d_{2x}\, c_{2x} \qquad [3]$$

The subscripts of S indicate the node and the direction of the resultant force (2x) and the node and direction of the unit displacement (1x).

These resultant forces are computed by applying unit displacements at each DOF in turn, which produces a 20 by 20 stiffness matrix. Each resultant force S is a coefficient of this matrix as shown in Figure 4.

The transfer element has been incorporated into a modified version of the computer program NONSAP (3). Input requires a description of fastener spacing and a fastener load-slip curve from which k_{ij} can be determined.

Displacement Prediction

Accurate estimates of diaphragm deflection are important in the design of wood buildings. Perhaps the most important reason is to control the deformation of supporting elements. The overstressing of vertical load-carrying

components caused by the deformation of a horizontal diaphragm could lead to building collapse within the allowable strength capacity of the horizontal diaphragm. Also, knowing the deflection of a diaphragm gives an estimate of diaphragm stiffness, which is necessary in calculating the distribution of lateral forces to the various vertical load-carrying components.

The deflection for a particular diaphragm can be quantified according to the following equation (2):

$$\Delta = \frac{5VL^3}{8EAb} + \frac{VL}{4Gt} + 0.188L\, e_n + \frac{\Sigma(\Delta_c x)}{2b} \qquad [5]$$

where

A = diaphragm deflection, in
V = shear, lb/lin ft
L = diaphragm length, ft
b = diaphragm width, ft
A = area of chord cross section, in^2
E = elastic modulus of chords, lb/in^2
G = shear modulus of plywood, lb/in^2
t = effective plywood thickness for shear, in
e = nail slip of calculated load per nail on interior panels, based on shear per foot divided by number of nails per foot
$\Sigma(\Delta_c x)$ = sum of individual chord-splice values, each multiplied by its distance in the nearest support

The first term of this equation represents bending deflection, the second shear deflection, the third nail slip, and the fourth deformation of chord splices (if they occur). In this form, this equation is valid only for uniform loading and simple support conditions. Note that the various terms have been corrected for the units shown.

Deflections computed with this equation and the finite element model were compared to experimentally measured deflections of a 16- by 48-ft plywood-sheathed diaphragm tested by Tissel and Elliott (10). Figure 5 shows the framing details and sheathing layout of this laterally loaded diaphragm. The results of model analysis are shown in Figure 6. The solid lines indicate the result of static load cycling to failure. The finite element model predicts displacements that are quite close to the experimental curve, although the model tends to underestimate diaphragm displacement at higher load levels. This is to be expected since the model does not account for chord-splice slip, which occurred in the tested diaphragm. Bolted splices in diaphragm chords will slip when loaded, increasing overall diaphragm displacement.

Several other diaphragm sizes and types were analyzed for model verification. The results of these analyses have been submitted for publication (5).

The deflection equation also satisfactorily predicts diaphragm displacement but only at lower diaphragm shear-load levels. The term accounting for nail slip in Equation [5] was derived assuming a relationship between nail slip and shear deflection. It was assumed that the ratio of total elongation along the diagonal of each individual panel of plywood to total deflection of the diaphragm caused by shear is equivalent to the ratio of joint deformation of each panel to total diaphragm deflection caused by nail slip. This relationship is only accurate as long as the load per nail to nail slip relationship is linear, which limits the accurate use of this equation to lower levels of nail load. As a result, at higher diaphragm shear-load levels, the equation will tend to overestimate diaphragm displacement. This behavior is apparent in Figure 6. In the design of diaphragms, displacements are typically computed at design load levels where nonlinearity of nail slip is probably not evident. Even if it is, the equation errors are on the conservative side. However, future designs of wood structures using a reliability-based design format may require a definition of serviceability strain limits for which a complete description of diaphragm displacement will need to be known. The finite element model can provide this description.

Conclusions

The finite element model presented in this report can be used to analyze the nonlinear load displacement of wood diaphragms. Various geometries, sheathing types, and fastener spacings can be investigated with this model.

Analysis of a 16- by 48-ft horizontal diaphragm indicates good agreement up to the ultimate load of the diaphragm. Prediction of displacement with a commonly used diaphragm deflection equation also indicates good agreement, although this agreement is limited to lower load levels.

References

1. Amana, E. J., and L. G. Booth. 1967. Theoretical and experimental studies of nailed and glued plywood stress-skinned components: Part 1, theoretical study. J. Inst. Wood Sci. 4(1):43-69.

2. Applied Technology Council. 1981. Guidelines for the design of horizontal wood diaphragms. Report ATC-7. September.

3. Cheung, C. K. 1984. NONDIA--A structural analysis program for the static and dynamic response of nonlinear nailed wood diaphragm systems (modified from NONSAP). Dep. of Civ. Eng., Washington State University, Pullman, WA.

4. Easley, J. T., M. Foomani, and R. H. Dodds. 1982. Formulas for wood shear walls. J. Struct. Eng., ASCE 108(ST11):2460-2478.

5. Falk, R. H., and R. T. Itani. 1988. Finite element modeling of wood diaphragms. Accepted for publication in J. Struct. Eng., ASCE.

6. Foschi, R. O. 1977. Analysis of wood diaphragms and trusses. Part I: Diaphragms. Can. J. Civ. Eng. 4(3):345-352.

7. Itani, R. Y., and C. K. Cheung. 1984. Nonlinear analysis of sheathed wood diaphragms. J. Struct. Eng., ASCE 110(9):2137-2147.

8. McCutcheon, M. 1985. Racking deformations in wood shear walls. J. Struct. Eng., ASCE 111(2):257–269.

9. Petersen, J. 1983. Bibliography on lumber and wood panel diaphragms. J. Struct. Eng., ASCE109(12):2838-2852.

10. Tissel, J. R., and J. R. Elliott. 1977. Plywood diaphragms. Res. Rep. 138. Am. Plywood Assoc.

11. Tuomi, R. L., and W. J. McCutcheon. 1978. Racking strength of light frame nailed walls. J. Struct. Div., ASCE 104(ST7):1131-1140.

Table 1.--FUNCTIONS DESCRIBING SPRING PAIR DISPLACEMENT.

Displacement in terms of element height	Displacement in terms of element width
$d_{1x}(y) = 1 - 3a_j^2 + 2a_j^3$	$c_{1x}(x) = b_i$
$d_{1y}(y) = 1 - 3a_j^2 + 2a_j^3$	$c_{1y}(x) = b_i$
$d_{1\theta}(y) = [-a_j + 2a_j^2 - a_j^3]H$	$c_{1\theta}(x) = b_i$
$d_{2x}(y) = 3a_j^2 - 2a_j^3$	$c_{2x}(x) = b_i$
$d_{2y}(y) = 3a_j^2 - 2a_j^3$	$c_{2y}(x) = b_i$
$d_{2\theta}(y) = a_j^2 - a_j^3$	$c_{2\theta}(x) = b_i$
$d_{3x}(y) = 3a_j^2 - 2a_j^3$	$c_{3x}(x) = 1 - b_i$
$d_{3y}(y) = 3a_j^2 - 2a_j^3$	$c_{3y}(x) = 1 - b_i$
$d_{3\theta}(y) = a_j^2 - a_j^3$	$c_{3\theta}(x) = 1 - b_i$
$d_{4x}(y) = 1 - 3a_j^2 + 2a_j^3$	$c_{4x}(x) = 1 - b_i$
$d_{4y}(y) = 1 - 3a_j^2 + 2a_j^3$	$c_{4y}(x) = 1 - b_i$
$d_{4\theta}(y) = [-a_j + 2a_j^2 - a_j^3]H$	$c_{4\theta}(x) = 1 - b_i$
$d_{5x}(y) = 1 - a_j$	$c_{5x}(x) = b_i$
$d_{5y}(y) = 1 - a_j$	$c_{5y}(x) = b_i$
$d_{6x}(y) = a_j$	$c_{6x}(x) = b_i$
$d_{6y}(y) = a_j$	$c_{6y}(x) = b_i$
$d_{7x}(y) = 1 - a_j$	$c_{7x}(x) = 1 - b_i$
$d_{7y}(y) = 1 - a_j$	$c_{7y}(x) = 1 - b_i$
$d_{8x}(y) = a_j$	$c_{8x}(x) = 1 - b_i$
$d_{8y}(y) = a_j$	$c_{8y}(x) = 1 - b_i$

a_j = y/H, where j indicates the jth spring pair in a column.

b_i = x/W, where i indicates the ith spring pair in a row.

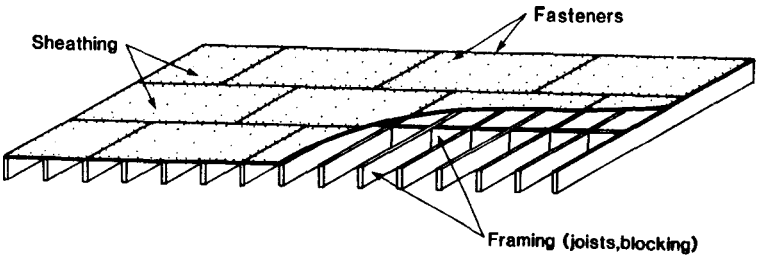

Figure 1.--Typical floor diaphragm. (ML11 5441)

Figure 2.--Transfer element. Nodes (1-8), degree of freedom (DOF), and coordinate orientation. H, height; W, width. (ML88 5439)

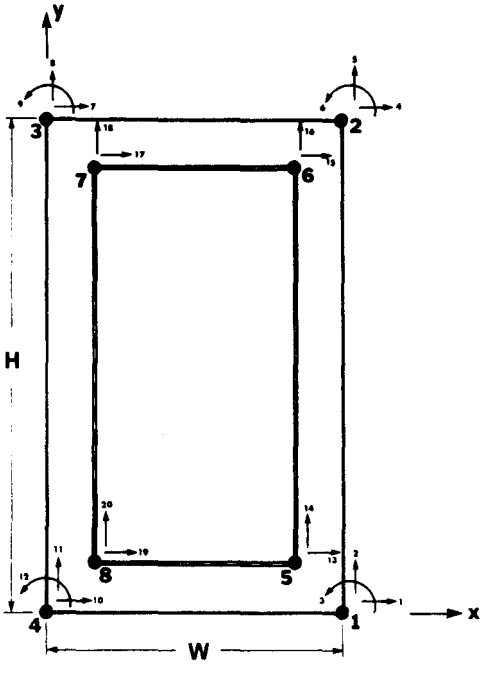

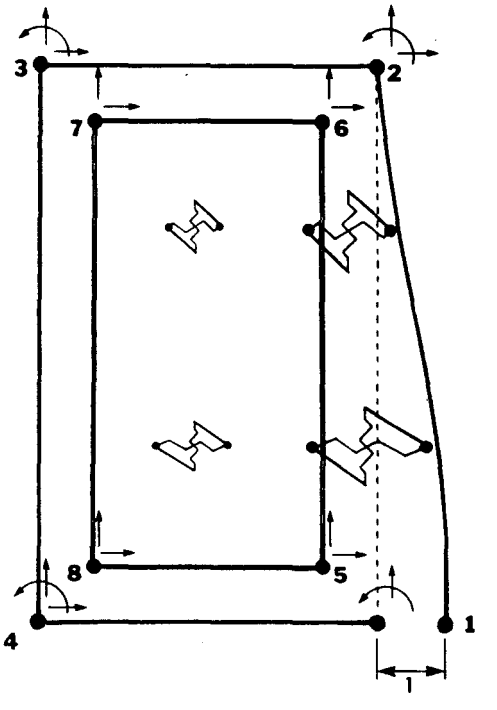

Figure 3.--Unit displacement of transfer element at DOF 1 and resulting spring pair elongation. (ML88 5440)

$$K_e = \sum_{i,j} k_{ij}$$

sym.

Figure 4.--Transfer element stiffness matrix.

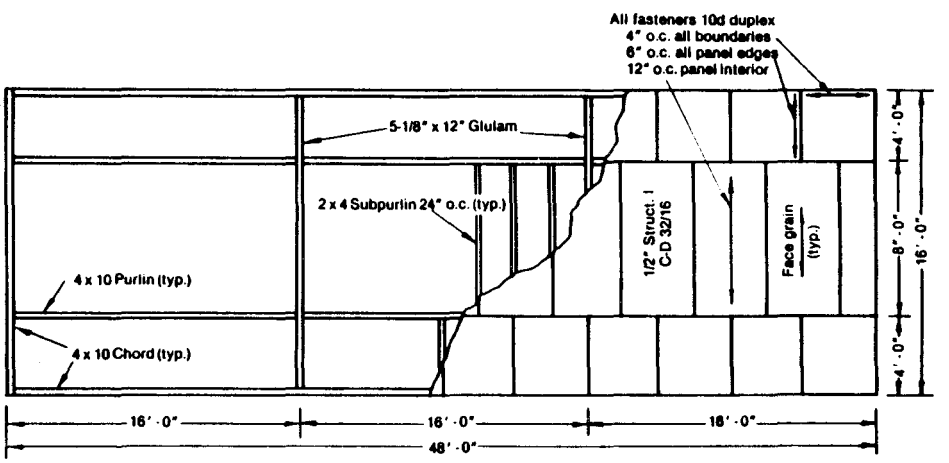

Figure 5.--The 16- by 48-ft diaphragm tested by Tissell and Elliott (10). Used with permission of the American Plywood Association. (ML88 5443)

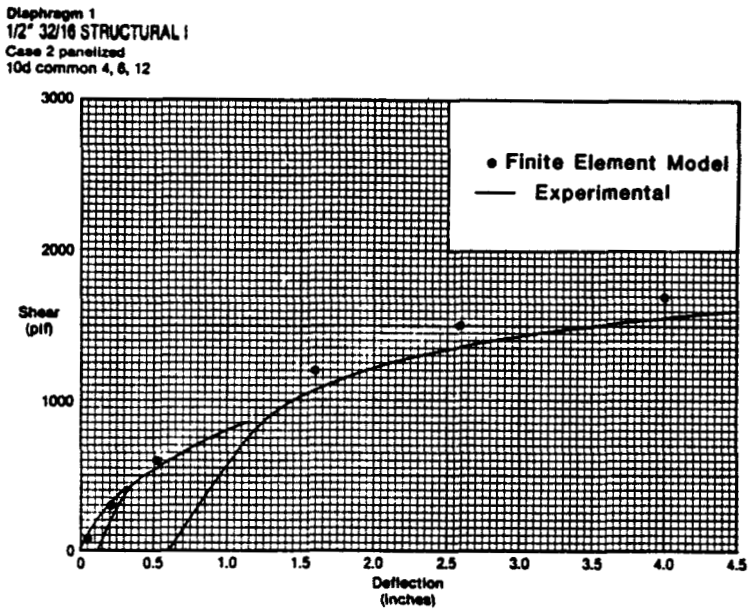

Figure 6.--Deflection equation and model analysis results for 16- by 48-ftdiaphragm (10). Used with permission of the American Plywood Association. (ML88 5442)

Proceedings of the

1988 INTERNATIONAL CONFERENCE ON TIMBER ENGINEERING

Editor

Rafik Y. Itani
Professor
WashingtonStateUniversity

Westin Hotel
Seattle, Washington
U.S.A.

September 19-22,1988

VOLUME 1

1988 INTERNATIONAL CONFERENCE ON TIMBER ENGINEERING

This proceedings includes papers presented at the 1988 International Conference on Timber Engineering which was held September 19-22, 1988 in Seattle, Washington, U.S.A. These papers are printed directly from camera ready manuscripts prepared by the authors. Views presented in the various papers are those of the respective authors and do not necessarily reflect those of the sponsors.

Editor

Rafik Y. Itani

Host Institution

Washington State University

Forest Products Research Society
2801 Marshall Court
Madison, Wisconsin 53705
(608) 231-1361; Fax: (608) 231-2152